Tactile-based Blind Grasping: Trajectory Tracking and Disturbance Rejection For In-Hand Manipulation of Unknown Objects

Wenceslao Shaw-Cortez, Denny Oetomo, Chris Manzie, and Peter Choong

***Abstract*— Tactile-based blind grasping refers to a realistic grasping scenario where the robotic hand has no knowledge of the object, and only has access to on-board sensors. This scenario is representative of real-world applications (e.g prosthetics) where high resolution cameras and other external sensors are not available to the robotic hand as they would be in a structured, laboratory setting. At present, there is no manipulation control that can track a reference object trajectory in tactile-based blind grasping. In this paper, a robust trajectory tracking controller is proposed to enhance the manipulation capabilities of robotic hands in tactile-based blind grasping. The proposed control ensures semi-global practical asymptotic tracking of the reference trajectory, while compensating for bounded wrench disturbances. Numerical simulations show the efficacy of the proposed approach.**

I. Introduction

Originally, robotic hand-based object manipulation was motivated by real-world applications including prosthetics, manipulation in hostile environments, and autonomous manipulation [1]. One type of object manipulation is in-hand manipulation where the robotic hand translates/rotates the object within the grasp, while compensating for disturbances that may act on the hand-object system. Trajectory tracking for in-hand manipulation refers to tracking a reference object pose trajectory. For the prosthetic example, trajectory tracking allows amputees to write and use hand tools effectively.

Although motivated by real-world applications, much of the existing work in object manipulation requires exact knowledge of the object being grasped [2], [3]. This paper addresses the real-world motivation by focusing on tactile-based blind grasping. In tactile-based blind grasping, the robotic hand is restricted to on-board sensing, with no a priori knowledge of the object. Thus the grasp properties including object center of mass, object mass, and external force/torques acting on the hand and/or object are uncertain. The restriction to on-board sensing eliminates motion capture systems and cameras that generally are not available outside a laboratory setting. On-board sensors include joint angle sensors and tactile sensors that can be integrated into the robotic hand [4].

Most literature in trajectory tracking for in-hand manipulation is restricted to situations when object information is known a priori, and is not applicable in tactile-based blind grasping [2], [3]. Robust feedback linearization [5], linearization [6], and adaptive control [7] methods require object pose measurements, which are obtained by motion capture systems or by physically placing sensors on the object prior to manipulation [5]–[7]. Other techniques such as motion planning also require knowledge of the object model/pose measurements, and rely on conservative assumptions that the system is quasi-static [8], [9]. In tactile-based blind grasping, the robotic hand does not have access to motion capture systems, and it is impractical to first place sensors on objects prior to grasping them. Thus those methods that require object models or pose measurements do not address the problem considered here.

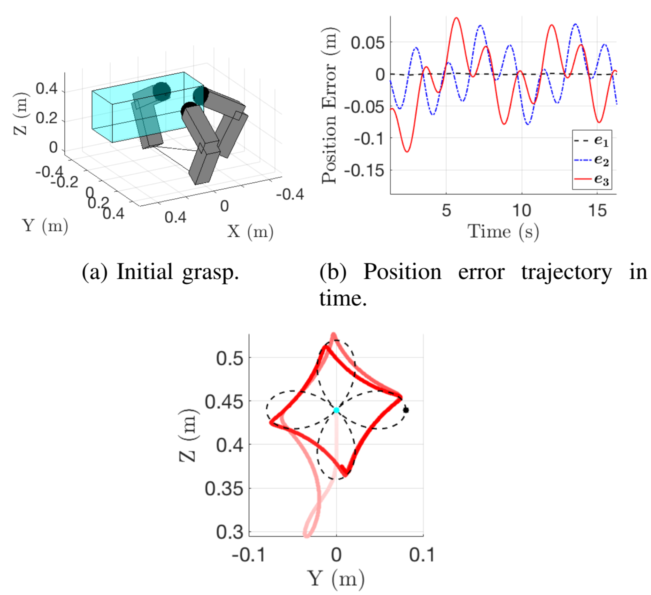

(a) Initial grasp.

(b) Position error trajectory in time.

(c) Reference (black-dash) and object (red) trajectories in space.

Fig. 1: Set-point manipulation control [10] for trajectory tracking results in large tracking error. In (c), the black dot indicates the initial position of the reference trajectory, and the cyan dot indicates the initial position of the object trajectory.

There exist solutions that only require on-board sensors, but are limited to set-point manipulation with assumptions that neglect hand-object dynamics/external disturbances [1], [11], [12]. Disturbances, such as gravity, and hand-object dynamics are inherent in object manipulation, but are unknown a priori due to the lack of object information. Ignoring

W. Shaw-Cortez, D. Oetomo, and C. Manzie are with the MIDAS Laboratory in the Department of Mechanical, Electrical, and Infrastructure Engineering, University of Melbourne, 3010, Australia, shaww@student.unimelb.edu.au, doetomo@unimelb.edu.au, manziec@unimelb.edu.au.

P. Choong is with the Department of Surgery, University of Melbourne, St. Vincent's Hospital, 3065, Australia, pchoong@unimelb.edu.au.

those effects compromise the stability of existing methods to tactile-based blind grasping considered here. Constant disturbances were addressed in [10], however that control was applicable only to set-point manipulation. Trajectory tracking allows for time-varying object references for more general, complex maneuvers. Set-point controllers could be applied for trajectory tracking by treating the time-varying reference as quasi-steady via a zero-order hold. Consider the hand holding an object (Figure 1a) with a gravity disturbance, and a reference rose curve trajectory. When a quasi-steady reference is tracked with the asymptotically stable, set-point manipulation control [10], the result, unsurprisingly, is a bounded error result with poor tracking performance as seen in Figures 1b and 1c. Thus the problem considered here is to determine a control law with the limited sensing from tactile-based blind grasping to track an in-hand manipulation trajectory with arbitrarily small tracking error.

In this paper, a manipulation controller is proposed to track an object reference trajectory, while simultaneously rejecting bounded disturbances for tactile-based blind grasping. The proposed method enhances the capabilities of robotic hands to compensate for external forces/torques and track time-varying references for more precise object manipulation. The proposed control guarantees semi-global practical asymptotic stability. Simulation results demonstrate the efficacy of the proposed controller.

Notation

Throughout this paper, the index i is specifically used to index over the n contact points in the grasp. An indexed vector $\boldsymbol{v}_i \in \mathbb{R}^p$ has an associated concatenated vector $\boldsymbol{v} \in \mathbb{R}^{pn}$. The notation $\boldsymbol{v}^{\mathcal{E}}$ indicates that the vector $\boldsymbol{v}$ is written with respect to a frame $\mathcal{E}$, and if there is no explicit frame defined, $\boldsymbol{v}$ is written with respect to the inertial frame, $\mathcal{P}$. $SO(3)$ denotes the special orthogonal group of dimension 3. The operator $(\cdot)\times$ denotes the skew-symmetric matrix representation of the cross-product. The Moore-Penrose generalized inverse of B is denoted $B^\dagger$. The $n \times n$ identity matrix is denoted $I_{n\times n}$.

II. Problem Formulation

A. Hand-Object System

Consider a fully-actuated, multi-fingered hand grasping a rigid, convex object at n contact points. The grasp consists of one contact point per finger with smooth, convex fingertips of high stiffness that each apply a contact force, $\boldsymbol{f}_{c_i} \in \mathbb{R}^3$, on the object. Let the hand configuration be defined by the joint angles, $\boldsymbol{q} \in \mathbb{R}^m$. The inertial frame, $\mathcal{P}$, is fixed on the palm of the hand, and a fingertip base frame, $\mathcal{F}_i$, is fixed at the point $\boldsymbol{p}_{f_i} \in \mathbb{R}^3$. The contact frame, $\mathcal{C}_i$, is located at the contact point, $\boldsymbol{p}_{c_i} \in \mathbb{R}^3$. The position vector from $\mathcal{F}_i$ to $\mathcal{C}_i$ is $\boldsymbol{p}_{fc_i} \in \mathbb{R}^3$. The contact geometry for the ith finger is shown in Figure 2. Let a fixed point on the fingertip surface be defined by $\boldsymbol{p}_{ft_i} \in \mathbb{R}^3$, which is fixed with respect to $\mathcal{F}_i$. The inertial position of this fixed point is $\boldsymbol{p}_{t_i} = \boldsymbol{p}_{f_i} + \boldsymbol{p}_{ft_i}$.

Let $\mathcal{O}$ be a reference frame fixed at the object center of mass $\boldsymbol{p}_o \in \mathbb{R}^3$, and $R_{po} \in SO(3)$ is the rotation matrix,

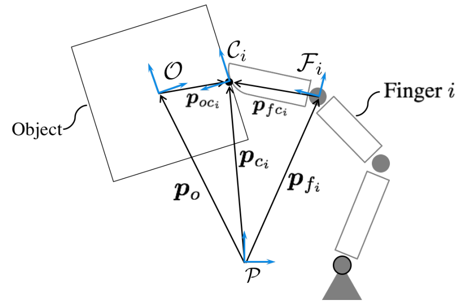

Fig. 2: A visual representation of the contact geometry for contact i.

which maps from $\mathcal{O}$ to $\mathcal{P}$. The object pose is defined by $\boldsymbol{x}_o \in \mathbb{R}^6$. The position vector from the object center of mass to the respective contact point is $\boldsymbol{p}_{oc_i} \in \mathbb{R}^3$.

The kinematics of the hand-object system are defined by the hand Jacobian and grasp map, respectively. The full Jacobian, J_h is constructed by combining each $J_{h_i}(\boldsymbol{q}_i, \boldsymbol{p}_{fc_i}) \in \mathbb{R}^{3\times m_i}$ into a block diagonal matrix [3]:

$$J_{h_i}(\boldsymbol{q}_i, \boldsymbol{p}_{fc_i}) = \begin{bmatrix} I_{3\times3} & -(\boldsymbol{p}_{fc_i})\times \end{bmatrix} J_{s_i}(\boldsymbol{q}_i) \tag{1}$$

where $J_{s_i}(\boldsymbol{q}_i) \in \mathbb{R}^{6\times m_i}$ is the manipulator Jacobian relating $\dot{\boldsymbol{q}}_i$ with the translational and rotational velocities about $\boldsymbol{p}_{f_i}$ [13]. The grasp map, $G(\boldsymbol{p}_{oc}) \in \mathbb{R}^{6\times 3n}$ is defined by [3]:

$$G(\boldsymbol{x}_o, \boldsymbol{p}_c) = \begin{bmatrix} I_{3\times3}, & \dots, & I_{3\times3}, \\ (\boldsymbol{p}_{c_1} - \boldsymbol{p}_o)\times, & \dots, & (\boldsymbol{p}_{c_n} - \boldsymbol{p}_o)\times \end{bmatrix} \tag{2}$$

Under the assumption that the object does not slip, the nonholonomic constraint that dictates the relation between the hand and object is [3]:

$$J_h \dot{\boldsymbol{q}} = G^T \dot{\boldsymbol{x}}_o \tag{3}$$

Note that for rolling contacts on smooth surfaces, $\boldsymbol{p}_c$ is a function of the hand configuration, object configuration, and geometry of the object and fingertip surfaces such that J_h and G can be expressed as functions of the hand-object state, $(\boldsymbol{q}, \boldsymbol{x}_o)$ [13].

The following assumptions are made for the grasp:

Assumption 1: The given hand has sufficient degrees of freedom such that $m = 3n$, and there exists a compact set $D_q \subset \mathbb{R}^m$ such that $\boldsymbol{q} \in D_q$ and D_q does not contain a singular hand configuration.

Assumption 2: The given multi-fingered grasp has $n > 2$ contact points, which are non-collinear.

Assumption 3: The fingertips roll, but do not slip, and the contact points remain on the fingertip surfaces.

Assumption 4: The fingertip and object surfaces at the contact points are locally smooth.

Remark 1: Assumption 1 ensures J_h is square and invertible, which is a common assumption in related work [6], [12]. This assumption is used to not distract from the main contribution here and can be relaxed by considering internal motion of the dynamics [13]. The existence of D_q is typically enforced by hardware restrictions, or can be actively ensured using constraint satisfaction techniques [14]. Assumption 2 ensures G is always full rank [3]. Assumption 3 ensures the nonholonomic grasp constraint (3) is satisfied,. No slip has previously been addressed by [15], which is also extendable to the control presented here.

Under Assumptions 1 and 3, the hand-object dynamics can be defined as [13]:

$$M_{ho}\ddot{\boldsymbol{x}}_o + C_{ho}\dot{\boldsymbol{x}}_o = GJ_h^{-T}\Big(\boldsymbol{u} + \boldsymbol{\tau}_e\Big) + \boldsymbol{w}_e \tag{4}$$

where $M_{ho} := M_{ho}(\boldsymbol{q}, \boldsymbol{x}_o) \in \mathbb{R}^{6\times6}$ is the hand-object inertia matrix, $C_{ho} := C_{ho}(\boldsymbol{q}, \dot{\boldsymbol{q}}, \boldsymbol{x}_o, \dot{\boldsymbol{x}}_o) \in \mathbb{R}^{6\times6}$ is the hand-object Coriolis and centrifugal matrix, $\boldsymbol{\tau}_e \in \mathbb{R}^m$ is the sum of all dissipative and non-dissipative disturbance torques acting on the joints, and $\boldsymbol{w}_e \in \mathbb{R}^6$ is an external wrench disturbing the object, and $\boldsymbol{u} \in \mathbb{R}^m$ is the joint torque control input for a fully actuated hand. Note M_{ho} and C_{ho} are smooth functions of their parameters [13].

Many existing solutions assume the disturbances $\boldsymbol{\tau}_e, \boldsymbol{w}_e$ to be zero, or exactly known so as to simply be canceled out [3], [6], [11]. In previous work that assumption was relaxed to account for constant disturbances for set-point manipulation [10]. This paper considers more general, bounded disturbances:

Assumption 5: The disturbances, $\boldsymbol{\tau}_e$, $\boldsymbol{w}_e$, are continuously differentiable, and $\boldsymbol{\tau}_e$, $\dot{\boldsymbol{\tau}}_e$ $\boldsymbol{w}_e$, and $\dot{\boldsymbol{w}}_e$ are bounded.

B. Task Frame Definition

In order to define the proposed control, a task frame must be used to substitute for the unknown object pose. In related work, it is common to define the task frame based on the hand configuration [11], [12]. Let $\mathcal{A}$ be the task frame located at the point $\boldsymbol{p}_a \in \mathbb{R}^3$ with respect to $\mathcal{P}$. Let $R_{pa} \in SO(3)$ be the rotation matrix mapping from frame $\mathcal{A}$ to $\mathcal{P}$. Let $\boldsymbol{v}_a \in \mathbb{R}^3$ denote the velocity of $\boldsymbol{p}_a$, and $\boldsymbol{\omega}_a \in \mathbb{R}^3$ denote the angular velocity of frame $\mathcal{A}$ with respect to $\mathcal{P}$. The task frame is defined by:

$$\boldsymbol{p}_a(\boldsymbol{q}) = \frac{1}{n}\sum_{i=0}^{n}\boldsymbol{p}_{t_i}(\boldsymbol{q}_i) \tag{5}$$

$$R_{pa}(\boldsymbol{q}) = [\boldsymbol{\rho}_x, \boldsymbol{\rho}_y, \boldsymbol{\rho}_z] \tag{6}$$

where $\boldsymbol{\rho}_x = \boldsymbol{\rho}_y \times \boldsymbol{\rho}_z, \boldsymbol{\rho}_y = \frac{\boldsymbol{p}_{t_1}-\boldsymbol{p}_{t_2}}{||\boldsymbol{p}_{t_1}-\boldsymbol{p}_{t_2}||_2}, \boldsymbol{\rho}_z = \frac{(\boldsymbol{p}_{t_3}-\boldsymbol{p}_{t_1})\times(\boldsymbol{p}_{t_2}-\boldsymbol{p}_{t_1})}{||(\boldsymbol{p}_{t_3}-\boldsymbol{p}_{t_1})\times(\boldsymbol{p}_{t_2}-\boldsymbol{p}_{t_1})||_2}$. A non-singular, local parameterization of R_{pa} is used to define the task frame orientation $\boldsymbol{\gamma}_a \in \mathbb{R}^3$, one example of which is $\boldsymbol{\gamma} =(\arctan(-\boldsymbol{\rho}_{z_2}/\boldsymbol{\rho}_{z_3}), \sqrt{1-\boldsymbol{\rho}_{z_1}^2}, \arctan(-\boldsymbol{\rho}_{y_1}/\boldsymbol{\rho}_{x_1}))$.

Let the task state be defined by $\boldsymbol{x} = (\boldsymbol{p}_a, \boldsymbol{\gamma}_a) \in \mathbb{R}^6$. To incorporate the local parameterization in the kinematics, let $S(\boldsymbol{\gamma}_a) \in \mathbb{R}^{3\times3}$ denote the one-to-one mapping defined by $\boldsymbol{\omega}_a = S(\boldsymbol{\gamma}_a)\dot{\boldsymbol{\gamma}}_a$. The matrix $S(\boldsymbol{\gamma}_a)$ is absorbed into $P(\boldsymbol{x}) = \text{diag}(I_{3\times3}, S(\boldsymbol{\gamma}_a))$ such that:

$$\begin{bmatrix} \dot{\boldsymbol{p}}_a \\ \boldsymbol{\omega}_a \end{bmatrix} = P(\boldsymbol{x})\dot{\boldsymbol{x}} \tag{7}$$

For notation, P will be used to denote $P(\boldsymbol{x})$.

Finally, let $\frac{\partial \boldsymbol{x}}{\partial \boldsymbol{q}} \in \mathbb{R}^{6\times m}$ denote the Jacobian of the task frame that maps $\dot{\boldsymbol{q}}$ to $\dot{\boldsymbol{x}}$. The following assumption is used in related work [11], [12]:

Assumption 6: The function $\boldsymbol{x}(\boldsymbol{q})$ is twice continuously differentiable, and $\frac{\partial \boldsymbol{x}}{\partial \boldsymbol{q}}$ is full rank.

C. Control Objective

The goal of object manipulation addressed here is to robustly track the reference trajectory, while compensating for external disturbances and system uncertainties associated with tactile-based blind grasping. Let $\boldsymbol{r}(t) \in \mathbb{R}^6$ denote the reference trajectory, and let $\boldsymbol{e} = \boldsymbol{x} - \boldsymbol{r}$ denote the error.

Assumption 7: The reference trajectory, $\boldsymbol{r}(t)$, is smooth and $\boldsymbol{r}, \dot{\boldsymbol{r}}, \ddot{\boldsymbol{r}}, \dddot{\boldsymbol{r}}$ are bounded.

This work focuses on achieving a practical form of stability that allows for sufficiently small tracking error for in-hand manipulation:

Definition 1: (Semi-global practical asymptotic stability) The system (4)) with state $\boldsymbol{\zeta} = (\boldsymbol{e}, \dot{\boldsymbol{e}})$ is semi-globally practically stable if there exists $\beta \in \mathcal{KL}$ such that for any $\Delta, \nu \in \mathbb{R}_{>0}$ there exists $\varepsilon^* \in \mathbb{R}_{>0}$ such that for all $\varepsilon \in (0, \varepsilon^*)$ the following holds:

$$|(\boldsymbol{\zeta})| \leq \beta(|\boldsymbol{\zeta}(0)|, t) + \nu, \quad \forall |(\boldsymbol{\zeta}(0))| < \Delta \tag{8}$$

The control problem addressed here is defined as follows:

Problem 1: Given a hand-object system that satisfies Assumptions 1-7, determine a control law that is semi-globally practically asymptotically stable with respect to the tracking error $(\boldsymbol{e}, \dot{\boldsymbol{e}})$.

III. Proposed Control

A. Trajectory Tracking Control Law

The proposed control law is defined by:

$$\boldsymbol{u} = \hat{J}_h^{\,T}\Big((P^T\hat{G})^{\dagger}\boldsymbol{u}_m + \boldsymbol{u}_f\Big) \tag{9}$$

$$\boldsymbol{u}_m = \hat{M}(\ddot{\boldsymbol{r}} - \hat{\boldsymbol{\eta}} - K_1\boldsymbol{e} - K_2\dot{\boldsymbol{e}}) \tag{10}$$

where $K_1, K_2 \in \mathbb{R}^{6\times6}$ are positive definite gain matrices, $\hat{M} \in \mathbb{R}^{6\times6}$ is a constant, positive-definite matrix, $\boldsymbol{u}_m \in \mathbb{R}^6$ is the manipulation controller, and $\boldsymbol{u}_f \in \mathbb{R}^{3n}$ is the internal force controller. The term $\hat{\boldsymbol{\eta}} \in \mathbb{R}^6$ is an estimate of the nonlinear disturbances of the hand-object system, whose update law is defined by:

$$\hat{\boldsymbol{\eta}} = \frac{1}{\varepsilon}(\boldsymbol{w} + \dot{\boldsymbol{e}}) \tag{11}$$

$$\dot{\boldsymbol{w}} = \ddot{\boldsymbol{r}} - \hat{M}^{-1}\boldsymbol{u}_m - \frac{1}{\varepsilon}(\boldsymbol{w} + \dot{\boldsymbol{e}}),\ \boldsymbol{w}(0) = -\dot{\boldsymbol{e}}(0) \tag{12}$$

where $\varepsilon \in \mathbb{R}_{>0}$.

The terms $\hat{J}_h \in \mathbb{R}^{3n\times m}$ and $\hat{G} \in \mathbb{R}^{6\times3n}$ are the respective approximations of J_h and G, and are solely defined as functions of the joint angles $\boldsymbol{q}$. The approximate hand Jacobian, $\hat{J}_h$, is a block diagonal matrix composed of $\hat{J}_{h_i}$:

$$\hat{J}_{h_i}(\boldsymbol{q}_i) = \begin{bmatrix} I_{3\times3} & -(\hat{\boldsymbol{p}}_{ft_i}(\boldsymbol{q}_i))\times \end{bmatrix}\hat{J}_{s_i}(\boldsymbol{q}_i) \tag{13}$$

where $\hat{J}_{s_i}$ refers to the approximate spatial Jacobian resulting from approximations in the link lengths and joint positions. The approximation $\hat{G}$ is defined as:

$$\hat{G}(\boldsymbol{q}) = \begin{bmatrix} I_{3\times3}, & ..., & I_{3\times3}, \\ (\hat{\boldsymbol{p}}_{t_1}(\boldsymbol{q}) - \boldsymbol{p}_a(\boldsymbol{q}))\times, & ..., & (\hat{\boldsymbol{p}}_{t_n}(\boldsymbol{q}) - \boldsymbol{p}_a(\boldsymbol{q}))\times \end{bmatrix} \tag{14}$$

The internal force control, $\boldsymbol{u}_f$, is responsible for ensuring the object does not slip during the manipulation motion. A common property of existing internal force controllers is summarized in the following assumption:

Assumption 8: The internal force control, $\boldsymbol{u}_f$ is continuously differentiable, and $\boldsymbol{u}_f$, $\dot{\boldsymbol{u}}_f$ are bounded.

One acceptable solution for the internal force control includes the centroid approach in which the fingertips are directed towards the centroid of the contact points [11] :

$$\boldsymbol{u}_f = k_f(\boldsymbol{p}_a - \boldsymbol{p}_{t_1}, \boldsymbol{p}_a - \boldsymbol{p}_{t_2}, ..., \boldsymbol{p}_a - \boldsymbol{p}_{t_n})^T \tag{15}$$

where $k_f \in \mathbb{R}_{>0}$ is a scalar gain. Note that if (15) is used to define $\boldsymbol{u}_f$, then the proposed control (9), (10) only requires proprioceptive measurements of $\boldsymbol{q}, \dot{\boldsymbol{q}}$. However, the internal force defined by (15) does not guarantee Assumption 3 holds.

A systematic way of defining $\boldsymbol{u}_f$ to ensure Assumption 3 holds is presented in [15]. That method is extendable to the control presented here by replacing the generalized inverse $(P^T\hat{G})^\dagger$ with the quadratic program formulation from [15], which is omitted here for brevity.

B. Stability Analysis

In the following analysis, the proposed control is proven to track the reference and compensate for bounded disturbances that arise in tactile-based blind grasping. Semi-global practical asymptotic stability of the hand-object system is achieved by exploiting existing work in high gain observers and control of robot manipulators [16], [17]. In the following derivation, the hand-object system dynamics is re-written in a singularly perturbed form, similar to that of [16].

To start, the system dynamics are derived for the state $\boldsymbol{x}$, by deriving the relation between $\dot{\boldsymbol{x}}$ and $\dot{\boldsymbol{x}}_o$. From Assumptions 1 and 3, $\dot{\boldsymbol{q}}$ is solved for from (3) and substituted into $\dot{\boldsymbol{x}} = \frac{\partial \boldsymbol{x}}{\partial \boldsymbol{q}}\dot{\boldsymbol{q}}$:

$$\dot{\boldsymbol{x}} = \frac{\partial \boldsymbol{x}}{\partial \boldsymbol{q}} J_h^{-1} G^T \dot{\boldsymbol{x}}_o \tag{16}$$

For ease of notation, let $J_a = \frac{\partial \boldsymbol{x}}{\partial \boldsymbol{q}} J_h^{-1} G^T$. Note that from Assumptions 1, 2, and 6, J_a is square and invertible such that $\dot{\boldsymbol{x}}_o = J_a^{-1}\dot{\boldsymbol{x}}$.

Lemma 1: Under Assumptions 1, 2, 3, 6, 7 and given a compact set $\Gamma \subset \mathbb{R}^{12}$, there exists a compact set $D_{x_o} \subset \mathbb{R}^6$ such that $\boldsymbol{x}_o \in D_{x_o}$ and there exists $v_1, v_2 \in \mathbb{R}_{>0}$ such that $\dot{\boldsymbol{q}}$ and $\dot{\boldsymbol{x}}_o$ respectively satisfy:

$$||\dot{\boldsymbol{q}}|| \leq v_1, \ \forall (\boldsymbol{e}, \dot{\boldsymbol{e}}) \in \Gamma \tag{17}$$

$$||\dot{\boldsymbol{x}}_o|| \leq v_2, \ \forall (\boldsymbol{e}, \dot{\boldsymbol{e}}) \in \Gamma \tag{18}$$

Proof: The existence of D_{x_o} follows from Assumptions 1 and 3, where due to the bounded $\boldsymbol{q}$, and restriction of the contact to the fingertip surface, the object pose must be bounded to within the hand workspace. By Assumptions 1, 2, and 6, J_a and $\frac{\partial \boldsymbol{x}}{\partial \boldsymbol{q}}$ are invertible such that $\dot{\boldsymbol{x}}_o = J_a^{-1}\dot{\boldsymbol{x}}$ and $\dot{\boldsymbol{q}} = \frac{\partial \boldsymbol{x}}{\partial \boldsymbol{q}}^{-1}\dot{\boldsymbol{x}}$. Substitution of $\dot{\boldsymbol{x}}$ with $\dot{\boldsymbol{e}} + \dot{\boldsymbol{r}}$, and boundedness of $\dot{\boldsymbol{r}}$ from Assumption 7 completes the proof. ■

To derive the dynamics for $\boldsymbol{x}$, $\dot{\boldsymbol{x}}_o = J_a^{-1}\dot{\boldsymbol{x}}$ is differentiated as follows:

$$\ddot{\boldsymbol{x}}_o = \frac{d}{dt}[J_a^{-1}]\dot{\boldsymbol{x}} + J_a^{-1}\ddot{\boldsymbol{x}} \tag{19}$$

Note a similar relation between $\ddot{\boldsymbol{q}}$ and $\ddot{\boldsymbol{x}}$ is derived by differentiating $\dot{\boldsymbol{q}} = \frac{\partial \boldsymbol{x}}{\partial \boldsymbol{q}}^{-1}\dot{\boldsymbol{x}}$:

$$\ddot{\boldsymbol{q}} = \frac{d}{dt}[\frac{\partial \boldsymbol{x}}{\partial \boldsymbol{q}}^{-1}]\dot{\boldsymbol{x}} + \frac{\partial \boldsymbol{x}}{\partial \boldsymbol{q}}^{-1}\ddot{\boldsymbol{x}} \tag{20}$$

Substitution of (19) into (4), left multiplication by J_a^{-T}, and substitution of $\boldsymbol{x} = \boldsymbol{e} + \boldsymbol{r}$ results in the following system dynamics:

$$M_a\ddot{\boldsymbol{e}} + C_a\dot{\boldsymbol{e}} = -M_a\ddot{\boldsymbol{r}} - C_a\dot{\boldsymbol{r}} + J_a^{-T}GJ_h^{-T}(\boldsymbol{u} + \boldsymbol{\tau}_e) + J_a^{-T}\boldsymbol{w}_e \tag{21}$$

where

$$M_a = J_a^{-T} M_{ho} J_a^{-1} \tag{22}$$

$$C_a = J_a^{-T} M_{ho} \frac{d}{dt}[J_a^{-1}] + J_a^{-T} C_{ho} J_a^{-1} \tag{23}$$

Note due to the change of variables, $M_a := M_a(\boldsymbol{e}, \boldsymbol{r}, \boldsymbol{q}, \boldsymbol{x}_o)$ and $C_a := C_a(\boldsymbol{e}, \dot{\boldsymbol{e}}, \boldsymbol{r}, \dot{\boldsymbol{r}}, \boldsymbol{q}, \dot{\boldsymbol{q}}, \boldsymbol{x}_o, \dot{\boldsymbol{x}}_o)$. It is straightforward to see that the inertia matrix M_a is positive definite and ultimately bounded due to the original properties of M_{ho} [13] and the full rank conditions of J_a, J_h, and G. This is summarized in the following lemma:

Lemma 2: Under Assumptions 1, 2, and 6, M_a defined by (22) is positive definite, and uniformly bounded.

The proposed control (9) is then substituted into (21), where the approximate matrix inverses in (9) are multiplied out by their exact terms resulting in residual disturbance terms. Note P is treated as an approximation of J_a^{-1}, which is motivated by the relations defined in (16) and (7) (i.e. $\dot{\boldsymbol{x}}_o$ is approximated by $(\dot{\boldsymbol{p}}_a, \boldsymbol{\omega}_a)$). This substitution results in:

$$M_a\ddot{\boldsymbol{e}} + C_a\dot{\boldsymbol{e}} = -M_a\ddot{\boldsymbol{r}} - C_a\dot{\boldsymbol{r}} + \boldsymbol{u}_m + J_a^{-T}GJ_h^{-T}\boldsymbol{\tau}_e + J_a^{-T}\boldsymbol{w}_e + D_1\boldsymbol{u}_m + D_2\boldsymbol{u}_f \tag{24}$$

where $D_1 := D_1(\boldsymbol{x}, \boldsymbol{q}, \boldsymbol{x}_o) \in \mathbb{R}^{6\times 6}$, $D_2 := D_2(\boldsymbol{x}, \boldsymbol{q}, \boldsymbol{x}_o) \in \mathbb{R}^{6\times 3n}$ represent the residual matrices that arise from the approximations of J_h, G, and J_a multiplying their respective inverses.

Let $\boldsymbol{\psi} \in \mathbb{R}^6$ denote the cumulative disturbance including the Coriolis and centrifugal terms:

$$\boldsymbol{\psi} = -C_a(\dot{\boldsymbol{e}} + \dot{\boldsymbol{r}}) + J_a^{-T}GJ_h^{-T}\boldsymbol{\tau}_e + J_a^{-T}\boldsymbol{w}_e + D_1\boldsymbol{u}_m + D_2\boldsymbol{u}_f \tag{25}$$

Furthermore, let $\boldsymbol{\eta} \in \mathbb{R}^6$ denote the full system nonlinearities defined by:

$$\boldsymbol{\eta} = M_a^{-1}\boldsymbol{\psi} + (M_a^{-1} - \hat{M}^{-1})\boldsymbol{u}_m \tag{26}$$

The system dynamics (24) is re-written using (25), (26), and (10)

$$\ddot{\boldsymbol{e}} = -K_1\boldsymbol{e} - K_2\dot{\boldsymbol{e}} + (\boldsymbol{\eta} - \hat{\boldsymbol{\eta}}) \tag{27}$$

Let $\boldsymbol{y} = \boldsymbol{\eta} - \hat{\boldsymbol{\eta}}$ denote the error between the nonlinear term $\boldsymbol{\eta}$ and the estimated term $\hat{\boldsymbol{\eta}}$. Differentiation of (11) with substitutions from (12) and (27) results in: $\dot{\hat{\boldsymbol{\eta}}} = \frac{1}{\varepsilon}\boldsymbol{y}$. Differentiation of (26) is omitted for brevity, and results in :

$$\dot{\boldsymbol{\eta}} = -\frac{1}{\varepsilon}(M_a^{-1}\hat{M} - I_{6\times 6})\boldsymbol{y} + \boldsymbol{\phi} \tag{28}$$

$$\phi = M_a^{-1}\Big(\dot{M}_a(K_1\boldsymbol{e} + K_2\dot{\boldsymbol{e}} - \boldsymbol{y})$$
$$-(\hat{M} - M_a)(\ddot{\boldsymbol{r}} + K_2K_1\boldsymbol{e} - K_1\dot{\boldsymbol{e}} + K_2K_2\dot{\boldsymbol{e}} + K_2\boldsymbol{y}) + \dot{\boldsymbol{\psi}}\Big) \tag{29}$$

Finally, the system dynamics for tactile-based blind grasping (21) is re-written in the following singularly perturbed form by combining (27) with $\dot{\boldsymbol{y}} = \frac{1}{\varepsilon}\boldsymbol{y} + \dot{\boldsymbol{\eta}}$ and (28):

$$\begin{bmatrix} \dot{\boldsymbol{e}} \\ \ddot{\boldsymbol{e}} \end{bmatrix} = A \begin{bmatrix} \boldsymbol{e} \\ \dot{\boldsymbol{e}} \end{bmatrix} + B\boldsymbol{y} \tag{30a}$$

$$\varepsilon\dot{\boldsymbol{y}} = -M_a^{-1}\hat{M}\boldsymbol{y} + \varepsilon\boldsymbol{\phi} \tag{30b}$$

where $A = \begin{bmatrix} 0_{6\times6} & I_{6\times6} \\ -K_1 & -K2 \end{bmatrix}$ and $B = \begin{bmatrix} 0_{6\times6} \\ I_{6\times6} \end{bmatrix}$. Let $V_r = \boldsymbol{\zeta}^T F \boldsymbol{\zeta}$ be the Lyapunov function of the reduced system (30a) where $\boldsymbol{\zeta} = (\boldsymbol{e}, \dot{\boldsymbol{e}})$, and F satisfies $FA + A^T F = -I_{6\times6}$. Furthermore let $V_{bl} = \boldsymbol{y}^T\boldsymbol{y}$ be the Lyapunov function for the boundary layer system (30b) for when (33) holds.

The system dynamics (30) is similar in form to that of [16], except for the disturbances in $\boldsymbol{\psi}$ that arise from tactile-based blind grasping and the dependence of M_a on the hand and object states. The following lemma ensures boundedness of $\boldsymbol{\phi}$:

Lemma 3: Under Assumptions 1-8, and given compact sets $\Gamma \subset \mathbb{R}^{12}$, $D_r \subset \mathbb{R}^{24}$ there exists $\nu_1, \nu_2 \in \mathbb{R}_{>0}$ such that $\boldsymbol{\phi}$ satisfies:

$$||\boldsymbol{\phi}|| \leq \nu_1 + \nu_2||\boldsymbol{y}||,\ \forall(\boldsymbol{e}, \dot{\boldsymbol{e}}) \in \Gamma, \boldsymbol{y} \in \mathbb{R}^6, (\boldsymbol{r}, \dot{\boldsymbol{r}}, \ddot{\boldsymbol{r}}, \dddot{\boldsymbol{r}}) \in D_r \tag{31}$$

Proof: From Assumption 1 and Lemma 1, it follows that bounded $(\boldsymbol{e}, \dot{\boldsymbol{e}})$ implies bounded states $\boldsymbol{q}, \boldsymbol{x}_o, \dot{\boldsymbol{q}}, \dot{\boldsymbol{x}}_o$. Thus with Assumptions 1, 4, 7, it follows that $\dot{M}_a$ is a continuous function on a compact set. Thus from (29) all terms apart from $\dot{\boldsymbol{\psi}}$ are either bounded or linear with respect to $\boldsymbol{y}$. To investigate $\dot{\boldsymbol{\psi}}$, $\boldsymbol{\psi}$ is differentiated:

$$\dot{\boldsymbol{\psi}} = \frac{\partial\boldsymbol{\psi}}{\partial\boldsymbol{e}}\dot{\boldsymbol{e}} + \frac{\partial\boldsymbol{\psi}}{\partial\dot{\boldsymbol{e}}}\ddot{\boldsymbol{e}} + \frac{\partial\boldsymbol{\psi}}{\partial\boldsymbol{r}}\dot{\boldsymbol{r}} + \frac{\partial\boldsymbol{\psi}}{\partial\dot{\boldsymbol{r}}}\ddot{\boldsymbol{r}} + \frac{\partial\boldsymbol{\psi}}{\partial\boldsymbol{q}}\dot{\boldsymbol{q}} + \frac{\partial\boldsymbol{\psi}}{\partial\dot{\boldsymbol{q}}}\ddot{\boldsymbol{q}}$$
$$+\frac{\partial\boldsymbol{\psi}}{\partial\boldsymbol{x}_o}\dot{\boldsymbol{x}}_o + \frac{\partial\boldsymbol{\psi}}{\partial\dot{\boldsymbol{x}}_o}\ddot{\boldsymbol{x}}_o + \frac{\partial\boldsymbol{\psi}}{\partial\boldsymbol{\tau}_e}\dot{\boldsymbol{\tau}}_e + \frac{\partial\boldsymbol{\psi}}{\partial\boldsymbol{w}_e}\dot{\boldsymbol{w}}_e + \frac{\partial\boldsymbol{\psi}}{\partial\boldsymbol{u}_m}\dot{\boldsymbol{u}}_m + \frac{\partial\boldsymbol{\psi}}{\partial\boldsymbol{u}_f}\dot{\boldsymbol{u}}_f \tag{32}$$

From boundedness of $\boldsymbol{e}, \dot{\boldsymbol{e}}, \boldsymbol{q}, \boldsymbol{x}_o, \dot{\boldsymbol{q}}, \dot{\boldsymbol{x}}_o$ and Assumptions 5, 7, and 8, all $\frac{\partial\boldsymbol{\psi}}{\partial\cdot}$ are continuous functions over compact sets. With Assumptions 5, 7, 8, it is clear that the terms in (32) apart from $\ddot{\boldsymbol{q}}$, $\ddot{\boldsymbol{x}}_o$, $\dot{\boldsymbol{u}}_m$, and $\ddot{\boldsymbol{e}}$ are bounded. Substitution of (20) and (19) in (32) replaces dependency of $\ddot{\boldsymbol{q}}$ and $\ddot{\boldsymbol{x}}_o$ with $\ddot{\boldsymbol{x}} = \ddot{\boldsymbol{e}} + \ddot{\boldsymbol{r}}$. Differentiation of $\boldsymbol{u}_m$ results in $\dot{\boldsymbol{u}}_m = \hat{M}(\dddot{\boldsymbol{r}} - \frac{\boldsymbol{y}}{\varepsilon} - K_1\dot{\boldsymbol{e}} - K_2\ddot{\boldsymbol{e}})$, which leaves only terms related to $\ddot{\boldsymbol{e}}$ and $\boldsymbol{y}$. Substitution of (30a) for all remaining $\ddot{\boldsymbol{e}}$ terms shows linear dependence on $\boldsymbol{y}$ with all remaining terms bounded, and completes the proof. ■

For stability of the singularly perturbed system, the matrix $\hat{M} \in \mathbb{R}^{6\times6}$ must satisfy:

$$||I_{6\times6} - M_a^{-1}\hat{M}|| < 1 \tag{33}$$

Existence of such an $\hat{M}$ that satisfies (33) is guaranteed in the following lemma:

Lemma 4: Under Assumptions 1, 2, 6, there exists a constant $\hat{M}$ such that (33) is always satisfied.

Proof: Assumptions 1, 2, 6 ensure M_a is uniformly bounded from Lemma 2, and the proof follows from [18]. ■

Remark 2: The existence of $\hat{M}$ for any M_a fits nicely into the tactile-based blind grasping setting in which the object mass is unknown to the on-board controller. As discussed in [16], [18], an acceptable $\hat{M}$ to satisfy (33) is $\hat{M} = \frac{1}{c}I_{6\times6}$ where $c = (m_{max} + m_{min})/2$ and $m_{max}, m_{min} \in \mathbb{R}_{>0}$ refer to the upper and lower bounds, respectively, on M_a. Thus for practical implementation the proposed controller only requires upper and lower bounds for M_a.

The following theorem ensures semi-global practical asymptotic stability to the reference for tactile-based blind grasping:

Theorem 1: Under Assumptions 1- 8 the system (21) with control law (9), (10) is semi-globally practically asymptotically stable with ultimate bound $\nu = \frac{\nu_1||FB||}{a/\varepsilon - c\nu_2}\sqrt{\frac{\lambda_{max}(F)}{\lambda_{min}(F)}}$ for $a, c \in \mathbb{R}$ where $a, c \in (0, 1)$.

Proof: Assumptions 5, 7 with Lemmas 2 and 3 satisfy the conditions from [16] such that semi-global practical stabilizability proof follows. The ultimate bound is computed similar to [17]. ■

The ultimate bound from Theorem 1 shows the trade-off between control and performance, which aligns with intuition. Large control gains, K_1, K_2 and a small ε improve the ultimate bound of the proposed control. However, larger magnitudes of $\boldsymbol{w}_e$, $\boldsymbol{\tau}_e$, $\dot{\boldsymbol{r}}$, $\ddot{\boldsymbol{r}}$, and $\dddot{\boldsymbol{r}}$ (i.e. larger ν_1), relate to an aggressive reference trajectory with degraded performance.

IV. Simulation Results

In this numerical simulation, the proposed control is used to track a trajectory, while the robotic hand holds an object subject to an unknown weight, $\boldsymbol{w}_e = (0, 0, -5, 0, 0, 0)$. The reference trajectory is defined by $\boldsymbol{r} = (0, r_y, r_z, 0, 0, 0) + \boldsymbol{x}(0)$ where $r_y = 0.08\cos(2t)\cos(t)$, $r_z = 0.08\cos(2t)\sin(t)$.

The simulation consists of a three-fingered hand with nine degrees of freedom with two revolute joints located at each finger base and one revolute joint connecting the two links of each finger. The links all share the same dimensions and mass properties. The hand consists of hemispherical fingertips each in contact with a rectangular prism object held by the hand. The simulations were performed using ode45 (Matlab 2018) with a simulation time of 15 seconds, and the internal force control (15) was used to define $\boldsymbol{u}_f$. The simulation parameters are listed in Table I, and the initial grasp configuration is shown in Figure 1a.

Figure 3 shows the resulting tracking error as the proposed control tracks the given reference trajectory for gain values of $\varepsilon = 0.001, 0.0001$. The plots show the the position error and orientation error converging to a bound about the origin. Decreasing values of ε result in improved tracking performance as promised from the practical asymptotic stability property.

TABLE I: Simulation Parameters

Link dimensions	0.05 m $\times$ 0.05 m $\times$ 0.3 m
Link mass	0.25 kg
Link moment of inertia	$\mathrm{diag}([0.0019, 0.0001, 0.0019])$ kgm^2
Fingertip radius	0.06 m
Object dimensions	0.260 m $\times$ 0.660 m $\times$ 0.260 m
Object mass	0.51 kg
Object moment of inertia	$\mathrm{diag}([0.0058, 0.0214, 0.0214])$ kgm^2
Initial $\boldsymbol{p}_o$	$[0.200, 0.00, 0.410]$ m
Initial $\boldsymbol{p}_a$	$[-0.046, 0.00, 0.440]$ m
k_f	10.0
K_1	$I_{6\times 6}$
K_2	$2.50 * I_{6\times 6}$
$\hat{M}$	$0.01 * I_{6\times 6}$

Note the initial displacement is largely due to the unknown object weight, which is then compensated for by the control. These plots show that the proposed control is able to track the error whilst rejecting the unknown disturbance acting on the hand/object for arbitrary tracking performance. This allows for improved tracking over existing set-point manipulation controllers with representative results shown in Figure 1.

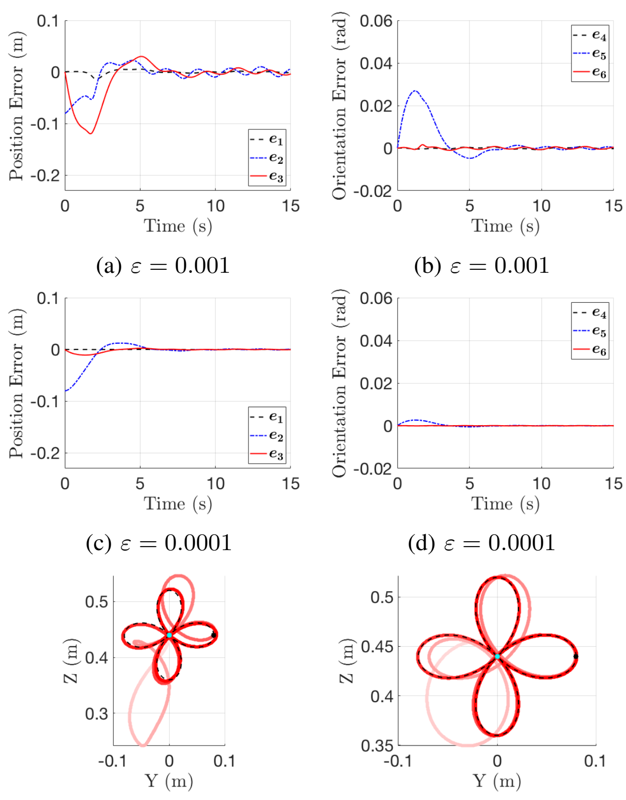

(a) $\varepsilon = 0.001$ (b) $\varepsilon = 0.001$

(c) $\varepsilon = 0.0001$ (d) $\varepsilon = 0.0001$

(e) $\varepsilon = 0.001$ (f) $\varepsilon = 0.0001$

Fig. 3: Tracking performance of the proposed control for $\varepsilon = 0.001, 0.0001$. The spatial representation of the reference (black-dash) and associated state trajectories, $\boldsymbol{p}_a$, (red) are spacially shown in (e) and (f).

The semi-global property of the controller ensures that, in theory, ε can be sufficiently decreased to achieve a desired tracking error. In practice, the choice of ε is dictated by noise sensitivities, which will incur a lower bound on ε. Also, high-gain observers are subject to the peaking phenomenon if ε is too low. The peaking phenomenon has been addressed by saturating the control to allow for small ε values [17].

V. Conclusion

In this paper, a robust trajectory tracking controller is proposed for object manipulation in tactile-based blind grasping. The proposed control guarantees semi-global practical asymptotic stability of the reference trajectory and compensates for uncertainties associated with unknown object properties and external wrenches. The analysis shows how tuning of the proposed method can achieve arbitrary tracking performance to the reference trajectory. Simulation results validate the efficacy of the proposed approach.

References

[1] R. Ozawa and K. Tahara, "Grasp and dexterous manipulation of multi-fingered robotic hands: A review from a control view point," *Adv. Robotics*, vol. 31, pp. 1030–1050, 2017.

[2] J. Kerr and B. Roth, "Analysis of multifingered hands," *Int. J. Robot. Res.*, vol. 4, no. 4, pp. 3–17, 1986.

[3] A. Cole, J. Hauser, and S. Sastry, "Kinematics and control of multifingered hands with rolling contact," *IEEE Trans. Autom. Control*, vol. 34, no. 4, pp. 398–404, 1989.

[4] Z. Kappassov, J. A. Corrales, and V. Perdereau, "Tactile sensing in dexterous robot hands - review," *Robot. Auton. Syst.*, vol. 74, pp. 195–220, 2015.

[5] Y. Fan, L. Sun, M. Zheng, W. Gao, and M. Tomizuka, "Robust dexterous manipulation under object dynamics uncertainties," in *Proc. IEEE Int. Conf. Adv. Int. Mechatronics*, 2017, pp. 613–619.

[6] A. Caldas, A. Micaelli, M. Grossard, M. Makarov, P. Rodriguez-Ayerbe, and D. Dumur, "Object-level impedance control for dexterous manipulation with contact uncertainties using an LMI-based approach," in *Proc. IEEE Int. Conf. Robot. Automat.*, 2015, pp. 3668–3674.

[7] S. Ueki, H. Kawasaki, T. Mouri, and A. Kaneshige, "Object manipulation based on robust and adaptive control by hemispherical soft fingertips," in *Proc. 18th IFAC World Congress*, vol. 18, 2011, pp. 14 654–14 659.

[8] M. Cherif and K. Gupta, "3D in-hand manipulation planning," in *Proc. IEEE/RSJ Int. Conf. Intel. Robot. Sys.*, vol. 1, 1998, pp. 146–151.

[9] K. Hertkorn, M. Roa, and C. Borst, "Planning in-hand object manipulation with multifingered hands considering task constraints," in *Proc. IEEE Int. Conf. Robot. Automat.*, 2013, pp. 617–624.

[10] W. Shaw-Cortez, D. Oetomo, C. Manzie, and P. Choong, "Robust object manipulation for prosthetic hand applications," in *IEEE Conf. Decision and Control*, 2017.

[11] K. Tahara, S. Arimoto, and M. Yoshida, "Dynamic object manipulation using a virtual frame by a triple soft-fingered robotic hand," in *Proc. IEEE Int. Conf. Robot. Automat.*, 2010, pp. 4322–4327.

[12] T. Wimböck, C. Ott, A. Albu-Schäffer, and G. Hirzinger, "Comparison of object-level grasp controllers for dynamic dexterous manipulation," *Int. J. Robot. Res.*, vol. 31, no. 1, pp. 3–23, 2012.

[13] R. Murray, Z. Li, and S. Sastry, *A mathematical introduction to robotic manipulation*. CRC Press: Boca Raton, FL, USA, 1994.

[14] W. Shaw-Cortez, D. Oetomo, C. Manzie, and P. Choong, "Grasp constraint satisfaction for object manipulation using robotic hands," in *IEEE Conf. Decision and Control*, 2018.

[15] W. Shaw Cortez, D. Oetomo, C. Manzie, and P. Choong, "Tactile-based blind grasping: A discrete-time object manipulation controller for robotic hands," *IEEE Robot. Autom. Lett.*, vol. 3, no. 2, 2018.

[16] I. Cervantes and J. Alvarez-Ramirez, "On the PID tracking control of robot manipulators," *Syst. Control Lett.*, vol. 42, no. 1, pp. 37–46, 2001.

[17] H. Khalil and L. Praly, "High-gain observers in nonlinear feedback control," *Int. J. of Robust and Nonlinear Control*, vol. 24, no. 6, pp. 993–1015, 2014.

[18] M. Spong, *Robot Dynamics and Control*. Wiley, 1989.